Front. Phys. 12(6), 126403 (2017)
DOI 10.1007/s11467-016-0633-y

RESEARCH ARTICLE

Renormalization group theory for temperature-driven first-order phase transitions in scalar models

Ning Liang, Fan Zhong†

State Key Laboratory of Optoelectronic Materials and Technologies, School of Physics, Sun Yat-sen University, Guangzhou 510275, China
Corresponding author. E-mail: †*stszf@mail.sysu.edu.cn*
Received August 23, 2016; accepted October 14, 2016

We study the scaling and universal behavior of temperature-driven first-order phase transitions in scalar models. These transitions are found to exhibit rich phenomena, though they are controlled by a single complex-conjugate pair of imaginary fixed points of ϕ^3 theory. Scaling theories and renormalization group theories are developed to account for the phenomena, and three universality classes with their own hysteresis exponents are found: a field-like thermal class, a partly thermal class, and a purely thermal class, designated, respectively, as Thermal Classes I, II, and III. The first two classes arise from the opposite limits of the scaling forms proposed and may cross over to each other depending on the temperature sweep rate. They are both described by a massless model and a purely massive model, both of which are equivalent and are derived from ϕ^3 theory via symmetry. Thermal Class III characterizes the cooling transitions in the absence of applied external fields and is described by purely thermal models, which include cases in which the order parameters possess different symmetries and thus exhibit different universality classes. For the purely thermal models whose free energies contain odd-symmetry terms, Thermal Class III emerges only at the mean-field level and is identical to Thermal Class II. Fluctuations change the model into the other two models. Using the extant three- and two-loop results for the static and dynamic exponents for the Yang–Lee edge singularity, respectively, which falls into the same universality class as ϕ^3 theory, we estimate the thermal hysteresis exponents of the various classes to the same precision. Comparisons with numerical results and experiments are briefly discussed.

Keywords first-order phase transitions, thermal phase transitions, renormalization group theory, ϕ^3 theory, scaling and universality, thermal classes, instability exponents, finite-time scaling, scalar model, dynamics, thermal hysteresis

PACS numbers 64.60.My, 75.60.Nt, 64.60.ae, 64.60.Bd

1 Introduction

Many first-order phase transitions (FOPTs) are driven to occur by varying the temperature T, and thermal hysteresis often ensues. Energy dissipation in processes studied using internal friction [1, 2] and thermal analysis [3–6] was found to follow a power law with respect to the sweep rate R of the temperature. On the basis of time-dependent Ginzburg–Landau theory of a $(\phi^2)^3$ model with $O(N)$ symmetry in the vector order parameter ϕ space in the limit of large components N, it was found that the areas A of the thermal hysteresis loops under a sinusoidally varying temperature depend on the amplitude r_a of the variation as $A = \oint M\mathrm{d}T \propto r_a^{\Upsilon}$ with a hysteresis exponent $\Upsilon = 1.0 \pm 0.03$ [7]. By using a linearly rather than sinusoidally varying temperature with a constant rate R, which is experimentally more amenable, familiar spindle-shaped thermal hysteresis loops of both the large-N $(\phi^2)^3$ and mean-field models were obtained [8]. In an entropy S versus T frame, the areas of the loops, which are proportional to the energy dissipation in the cycles, were found to be

$$A_2 = A_0 + aR^{\Upsilon}, \tag{1}$$

with $\Upsilon = 2/3$ independent of the model parameters, where A_0 and a are constants [8]. This dynamic hystere-

*arXiv: 1511.08258.

sis scaling including the exponent has been confirmed experimentally in a nematic–smectic-A phase transition of a binary mixture under a linearly varying temperature [9]. Recently, it was shown by using renormalization group (RG) theory that the FOPTs driven by an applied external field in a scalar ϕ^4 model *below* its critical temperature are controlled by the instability fixed point of a derived ϕ^3 model [10, 11]. Although it is imaginary in value, the fixed point is physical counter-intuitively if ϕ^3 theory is to be mathematically convergent [12]. Numerical evidence from the Potts model for the fixed point has also been found [13]. Functional RG theory has extended the theory to contain all odd-order terms and given rise to consistent exponents [14]. These then place the scaling behavior of the FOPTs in the same universality class as the Yang–Lee edge singularity [15], the singularity of the distribution of the Yang–Lee zeros *above* the critical point.

In ϕ^3 theory [10, 11], one first notices that, for an FOPT, there exists a sharply defined curve of spinodals for which the associated susceptibility diverges at the mean-field level that becomes exact for long-range interactions. Upon an expansion near them, these spinodals manifest themselves as the "critical" point of ϕ^3 theory, because the mean-field free energy now contains a ϕ^3 term as the leading coupling term even if the symmetry of the original theory excludes it. Because ϕ^3 theory is unstable at its critical point, we call it the instability point and the critical exponents characterizing it are referred to as instability exponents. Although one has a ϕ^3 theory for the unstable phenomena instead of the usual ϕ^4 one for critical phenomena, one can easily convince oneself, as will be seen in the following sections for temperature-driven transitions, that the whole theory for the latter applies to the former as well [11]. This includes the definitions (or the meaning) and computations of the mean-field instability exponents, the fluctuations that lead to a divergent correlation length, the Ginzburg criterion for the relative importance of the fluctuations, the shift of the instability point caused by the fluctuations, and RG theory for the non-Gaussian fixed point and its associated non-mean-field instability exponents, which combine to characterize the hysteresis near the instability point, as well as the irrelevance of the neglected higher order terms [11].

However, there exist several possible questions pertaining to ϕ^3 theory. The first concerns the physical meaning of the instability points and the existence of the spinodals. For a system with short-range interactions, it is generally believed that there exist no sharply defined spinodals, which contrasts with the mean-field case with long-range interactions [16–19]. This difference can be readily understood from the fact that thermal fluctuations simply smear out any possible spinodal in a region when the nucleation barrier is on the order of the thermal energy. By emphasizing the effect of the fluctuations nevertheless, the existence of a crossover between nucleation and spinodal decomposition is out of question as the former needs activation whereas the latter does not, at least away from the crossover region and at the early time of the transition. It is then more than natural to postulate the existence of hidden spinodals that, albeit smeared out again by thermal fluctuations, control the crossover. These hidden spinodals, which are shifted by the fluctuations away from their mean-field values, are nothing but the shifted instability points. Their magnitudes are nonuniversal and depend on the coarse-grain scale, in agreement with numerical results [16, 17, 20–24]. Although studies were performed in which the range of interactions was varied to approach the mean-field spinodals [25, 26], from the analogous ϕ^4 theory for criticality, it is clear that mean-field theory is only the correct starting point for the RG analysis of fluctuations in systems with short-range interactions. There is no apparent contradiction in describing the critical (unstable) behavior of a short-range-interaction system around a particular point existing only within the long-range-interaction mean-field models.

Another question pertains to the only prominent difference between ϕ^3 and ϕ^4 theories, i.e., that the fixed point of the former is imaginary in value. However, it has been found that, for a physical coupling of a purely real initial value, the RG flow has to diverge at a finite scale to achieve an imaginary part [11]. Combining a momentum-shell integration RG analysis and nucleation theory [27] near the spinodal point [28, 29] has shown that [12], exactly at the finite scale, the free-energy cost for nucleation out of the metastable state in which the system lies vanishes. So does the potential well of the metastable state itself. This places the system exactly at a true instability point and thus exhibits divergence at the finite scale. The integration for the partition function then diverges and has to be analytically continued to the complex plane to be physically meaningful. As a consequence, the system enters the imaginary domain and can thus reach the imaginary fixed point. Therefore, counter to the intuition that only real values are physical, for ϕ^3 theory, imaginary values are physical instead [12].

Yet another possible question concerns the relation to nucleation and growth [16–18, 30]. As the theory is an expansion around the instability points, it can apparently describe the behavior of spinodal decomposition [16, 17] at least at its early time. We note that, as the other dynamical mode of FOPTs, nucleation is the classical theory for FOPTs and has been argued to result in, for small R, a hysteresis that vanishes in a purely logarithmic form [31]. Although it has been shown un-

ambiguously that this nonperturbative nucleation effect can only play a role at extremely low rates that are not feasible experimentally [32, 33], no evidence of an overall power-law relationship has been found for the magnetic hysteresis in a sinusoidally oscillating field in two dimensions either [32, 33]. A direct consequence of nucleation theory is that the hysteresis loop ought to shrink and vanish in the limit of small rates. However, numerical simulations of the Ising model revealed the existence of a dynamic phase transition at finite amplitudes of the field, the transition below which the switch between the two phases of opposite magnetizations cannot take place [32–34]. It was even claimed that a finite field is needed to flip the magnetization even in the static limit of the field [34]. These results indicate that nucleation alone cannot explain the results and that the loci at which the dynamic transition occurs may well be the dynamic instability points even in the regime in which nucleation is thought to be dominant. The combination of RG and nucleation theories mentioned above shows that [12] the characteristic length scale at which the RG flows diverge and become imaginary divides the fluctuating field of a metastable system into two sets. The short modes feel a finite potential well and are responsible for nucleation, whereas the long ones feel none and are controlled by the imaginary fixed point. Although the short modes are renormalized away when coarse-grained and are thus irrelevant in the sense of RG theory, they may well compete with the long ones in a real system itself in which no renormalization is performed and mask the scaling behavior. Physically in a real system, when the time scale of nucleating out of the metastable state is shorter than the time of driving the system from, say, the equilibrium transition point to near the instability point, nucleation will probably occur. However, even near the instability point where nucleation barriers still exist owing to the ϕ^4 interaction that is irrelevant and neglected in ϕ^3 theory, nucleation may still play a role. Accordingly, disentangling nucleation from scaling in ϕ^3 theory has yet to be resolved. It is therefore helpful to turn to more examples.

Here, we shall develop RG theories for the dynamics of temperature-driven FOPTs in scalar models. We find that, although they are driven by varying the temperature instead of an external field, these FOPTs are again controlled by the same instability fixed point of ϕ^3 theory for field-driven transitions. Distinct from the latter case, however, there are now complicated behaviors. The temperature-driven FOPTs exhibit three universality classes with three sets of thermal hysteresis exponents: Thermal Classes I, II, and III correspond, respectively, to a field-like thermal class, a partly thermal class, and a purely thermal class. There is also a crossover between the first two classes. The last class can have further variants depending on the symmetry of the model. All these rich behaviors are clearly demonstrated from reduced models and well accounted for by RG theories.

In the following, we shall first study mean-field models for the thermal transitions in Section 2 and identify the three different universality classes in Section 3. Various reduced models for the different classes are also derived in the latter section. A scaling theory is then developed in Section 4 to account for the peculiar scaling behavior. RG theories for them follow in Section 5. A summary is given in Section 6.

2 Model

As a simple model that involves an FOPT between an ordered phase at low temperature and a disordered phase at high temperature, we consider the following free-energy functional [35, 36] in a d-dimensional space:

$$F[\phi]=\int \mathrm{d}\boldsymbol{r}\left(\frac{1}{2}r\phi^2+\frac{1}{2}[\nabla\phi]^2+\frac{1}{3!}w\phi^3+\frac{1}{4!}g\phi^4-H\phi z\right), \tag{2}$$

where r is a reduced temperature proportional to T, H is an external field conjugated to the scalar order parameter field ϕ, and w and g are coupling constants. For stability, $g>0$. Yet, w can be either positive or negative. For simplicity, we shall choose $w<0$ throughout, which results in an ordered phase with a positive equilibrium order parameter. Equation (2) contains a cubic term and thus ϕ has no inversion symmetry. If this symmetry is respected, however, a ϕ^6 term has to be included to have a thermal FOPT [37]. Nonetheless, it will be seen later that the transition is still governed by the same theory to be developed below except for the cooling transition when $H=0$, which belongs to the purely thermal class. We thus focus here on the model defined by Eq. (2).

Studying the transition driven to metastable states as the temperature is varied requires the dynamics to be considered. We employ pure relaxation dynamics of a nonconserved order parameter, i.e., Model A [38], described by the Langevin equation

$$\frac{\partial\phi}{\partial t}=-\lambda\frac{\delta F[\phi]}{\delta\phi}+\zeta, \tag{3}$$

where λ is a kinetic coefficient and the Gaussian white noise ζ satisfies

$$\begin{aligned}&\langle\zeta(\boldsymbol{r},t)\rangle=0,\\&\langle\zeta(\boldsymbol{r},t)\zeta(\boldsymbol{r}',t')\rangle=2\lambda T\delta(\boldsymbol{r}-\boldsymbol{r}')\delta(t-t'),\end{aligned} \tag{4}$$

and mimics the effect of other degrees of freedom, where the angle brackets denote averages over the noise.

3 Mean-field theory: Reduced models and thermal classes

3.1 Theory and reduced models

In the mean-field approximation, all fluctuations are ignored. As a result, $\langle\phi^k\rangle = M^k$ and Eq. (2) reduces to

$$\frac{\partial M}{\partial t} = -\lambda\left(rM - \nabla^2 M + \frac{1}{2!}wM^2 + \frac{1}{3!}gM^3 - H\right), \tag{5}$$

where we have kept the gradient term for later use though M is spatially uniform. In equilibrium and for $H = 0$, Eq. (5) describes an FOPT at an equilibrium transition temperature $r_e = w^2/(3g)$ at which M jumps from a disordered phase with $M = 0$ to an ordered phase with $M = M_e = (-3w + \sqrt{9w^2 - 24rg})/(2g)$. The stability limits or the spinodal points of the two phases lie at $(r_{s0}^-, M_{s0}^-) = (0, 0)$ and $(r_{s0}^+, M_{s0}^+) = (3w^2/(8g), -3w/(2g))$, respectively; these are solutions of

$$r_{s0}M_{s0} + \frac{1}{2}wM_{s0}^2 + \frac{1}{3!}gM_{s0}^3 - H = 0, \tag{6a}$$

$$r_{s0} + wM_{s0} + \frac{1}{2}gM_{s0}^2 = 0, \tag{6b}$$

with $H = 0$. We shall refer to the two spinodal points as cooling and heating spinodal/instability points, as they are relevant to cooling and heating transitions, respectively. For $H \neq 0$, below the critical point $H_c = -w^3/(6g^2)$, $r_c = w^2/(2g)$, and $M_c = -w/g$ given by Eq. (6) and the derivative of Eq. (6b) with M_{s0} (with all variables replaced by the critical ones), there are also FOPTs from a phase with small M to a phase with a large M. The spinodal points in this case are also determined by Eq. (6) [8].

Because there are no fluctuations, the dynamic FOPTs described by Eq. (5) can only take place beyond (r_{s0}, M_{s0}), as shown in the inset of Fig. 1, because at the spinodal, the barrier between the two phases vanishes and the system becomes unstable. Accordingly, we set

$$M(t) = M_{s0} + m(t), \tag{7}$$

and $m(t)$ is then described by the dynamics

$$\frac{\partial m}{\partial t} = -\lambda\left(\tau m - \nabla^2 m + \frac{1}{2!}vm^2 - K\right), \tag{8}$$

with

$$\tau = r + wM_{s0} + \frac{1}{2}gM_{s0}^2 = r - r_{s0}, \tag{9a}$$

$$K = H - rM_{s0} - \frac{1}{2}wM_{s0}^2 - \frac{1}{3!}gM_{s0}^3 = -M_{s0}\tau, \tag{9b}$$

$$v = w + gM_{s0}, \tag{9c}$$

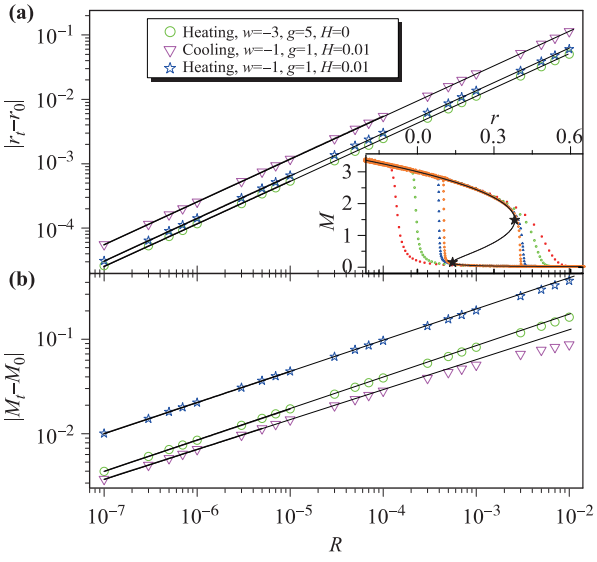

Fig. 1 Dependence of **(a)** the transition temperature r_t and **(b)** the transition order parameter M_t on the temperature sweep rate R. The thick lines are fits to the data covered and the thin lines are their direct extensions. The fitted lines have slopes 0.6649(2), 0.6645(8), 0.664(2) and intercepts 0.1379148(3), 0.3816972(3), 0.674999(4) in (a) and 0.3286(3), 0.3303(2), 0.3167(8) and 1.48627(2), 0.899960(6), 0.14917(2) in (b) from up to down. The corresponding theoretical slopes are 2/3 in (a) and 1/3 in (b), and the corresponding theoretical intercepts are 0.1379139, 0.3816968, 0.675 in (a) and 1.48642, 0.9, 0.149017 in (b). Inset: Hysteresis loops for several R of the parameter set with a finite field. The two black stars mark the spinodal/instability points. The curve connecting the two spinodal points is obtained from Eq. (6a).

near (r_{s0}, M_{s0}) from Eqs. (5) and (6). Note that, although Eq. (9) is exact, in Eq. (8), we have kept only the leading m^2 term and neglected the higher order m^3 term for (r, M) sufficiently near (r_{s0}, M_{s0}) and hence small τ and m. As a consequence, the free-energy functional responsible for Eq. (8) is a ϕ^3 theory in an effective field K. Therefore, the dynamics of the temperature-driven FOPTs near their instability points $\tau = 0$ and $K = 0$ is governed by ϕ^3 theory similar to the field-driven FOPTs.

ϕ^3 theory bears a particular symmetry that simplifies it. The model as defined in Eq. (8) appears to have two parameters, τ and K, for controlling its distance to the instability point. However, it is well known that there is only one independent parameter for ϕ^3 theory [15]. Indeed, since a shift of the order parameter by a constant amount c, i.e.,

$$m = \varphi - c, \tag{10}$$

only changes

$$m \to \varphi, \quad \tau \to \tau' = \tau - vc, \tag{11a}$$

$$K \to K' = K + \tau c - \frac{1}{2}vc^2, \tag{11b}$$

and thus keeps the structure of Eq. (8), a particular choice of c can turn the mass term τ into the effective-field term K and vice versa [39]. Accordingly, we have two equivalent reduced ϕ^3 theories to describe the thermal transitions.

The first one is a massless model of

$$\frac{\partial\varphi}{\partial t} = -\lambda\left(-\nabla^2\varphi+\frac{1}{2!}v\varphi^2 - \overline{K}\right), \tag{12}$$

with a shifted effective field (denoted by an overline)

$$\overline{K} = K + \tau^2/(2v) = -M_{s0}\tau + \tau^2/(2v) \tag{13}$$

for $c = \tau/v$.

The second is a purely massive model of

$$\frac{\partial\varphi}{\partial t} = -\lambda\left(\overline{\tau}\varphi - \nabla^2\varphi+\frac{1}{2!}v\varphi^2\right), \tag{14}$$

with a shifted mass satisfying

$$\overline{\tau}^2 = \tau^2 + 2vK = \tau(\tau - 2vM_{s0}) \tag{15}$$

for $c = \tau/v + \sqrt{\tau^2+2vK}/v$. However, this massive model is real only near the cooling spinodals (r_{s0}^-, M_{s0}^-) for $H = 0$. This can be seen as follows. From Eq. (9c), we see that, for $M_{s0} = M_c$, $v(M_c) = 0$. Because the heating and the cooling spinodals merge at M_c and are all positive for $w < 0$, for the heating spinodals, $M_{s0} > M_c$ and so $v > 0$ and hence $2vM_{s0} > 0$. whereas, for the cooling spinodals, $M_{s0} < M_c$ and thus $v < 0$ and hence $2vM_{s0} < 0$. The heating spinodals are the stability limits of the ordered phases and are relevant for the heating transitions. This means that $r > r_{s0}$ and $\tau > 0$ near the heating spinodals. A positive $2vM_{s0}$ then implies that $\overline{\tau}^2$ must be negative for sufficiently small heating rates and hence a sufficiently small τ from Eq. (15). Indeed, for $H = 0$, for instance, a direct computation gives $2vM_{s0}^+ = 4r_{s0}^+ > 0$ and $\overline{\tau}^2 = (r - r_{s0}^+)(r - 5r_{s0}^+)$, which is negative for the physically relevant range of $r_{s0}^+ < r < 5r_{s0}^+$. In contrast, the cooling spinodals are relevant for the cooling transitions and thus $r < r_{s0}$ and $\tau < 0$ near them. As a result, a negative $2vM_{s0}$ implies that $\overline{\tau}^2$ must be again negative for sufficiently small cooling rates. Yet, there is a special case in which $\overline{\tau}$ is real. This is the case for the cooling spinodals for $H = 0$, in which $M_{s0}^- = 0$ and thus $\overline{\tau}$ is simply τ. Consequently, Eq. (14) is just Eq. (5) with the cubic term omitted. Also, in this case, $c = 0$, which is the reason why we have kept only the plus sign for it. We see therefore that most of the temperature-driven transitions in the mean-field theory cannot be cast into a purely massive theory with real parameters. Nevertheless, we still study it because, when it is multiplied by the imaginary unit i, it can be formally changed to the theory of the Yang–Lee edge singularity, which falls into the same universality class as mentioned.

The foregoing discussions indicate that, besides the two equivalent reduced models (12) and (14), there exists another purely massive model

$$\frac{\partial\varphi}{\partial t} = -\lambda\left(\tau\varphi - \nabla^2\varphi+\frac{1}{2!}v\varphi^2\right), \tag{16}$$

which we call the purely thermal model. The only difference between the two purely massive models is that the mass term is τ instead of $\overline{\tau}$ for the purely thermal model because the order parameter at the instability point vanishes. As mentioned, the model (16) describes the cooling transition when $H = 0$ in the mean-field approximation. However, we shall see below that this is true only for the mean field. When fluctuations are taken into account, an effective field K is generated. As a consequence, we have to resort to the other two models.

The purely thermal model (16) can be generalized to a general form,

$$\frac{\partial\varphi}{\partial t} = -\lambda\left(\tau\varphi - \nabla^2\varphi+\frac{1}{\sigma!}v\varphi^\sigma\right), \tag{17}$$

with an integer σ. For $\sigma = 2$, the purely thermal model above is recovered. For $\sigma = 3$, however, the model describes the cooling transition of the ϕ^6 model for $H = 0$. It is also equivalent to the usual ϕ^4 model for continuous phase transitions [40]. We thus expect the two models with a different σ to fall into different universality classes. It is straightforward to extend the analysis to larger values of σ, but we shall not consider them further.

If Gaussian noise (4) is reintroduced, all four reduced models can describe the fluctuations near the instability points. The massless model was studied in Refs. [10, 11] and the equilibrium properties of the purely thermal model was investigated in Ref. [12]. For temperature-driven FOPTs, however, the controlling parameter in the first two models is a nonlinear function of τ, the reduced temperature to the instability point. We shall see that it is this nonlinearity that leads to the complication of the dynamic scaling for such transitions. The purely thermal model with an even σ in the presence of fluctuations also returns to the first two models. Only the generalized purely thermal model with an odd σ has simple behavior because of its lack of nonlinearity. In fact, it gives rise to the purely thermal class of Thermal Class III, which also results from the purely thermal model with an even σ in the mean field, whereas the first two models result in the other two classes and their crossover in some special limits. In the following, when we consider the purely massive models, we mainly consider Eq. (14), as the results for the purely thermal model Eq. (16) can be obtained by direct replacements.

We emphasize that the reduced models can describe the thermal transitions effectively because they only contain one controlling parameter. The general model (8) explicitly contains one redundant parameter, and care has to be executed when it is used.

3.2 Thermal classes

We identify the thermal classes in this subsection from numerical and some possible analytical results.

3.2.1 Field-like Thermal Class I

The usual dynamic scaling described by Eq. (1) with $\Upsilon = 2/3$ for the field-like Thermal Class I can be readily found from finite-time scaling (FTS) using a linearly varying temperature [41, 42] by numerically solving Eq. (5) with $r = r_{s0} + Rt$. We have purposely chosen the time origin at the instability point for simplicity. In fact, once it is sufficiently far away from r_{s0}, the initial r and hence the time origin have no effect on the scaling. The reduced transition temperature r_t characterized by r at $M = M_{s0}$ follows

$$r_t = r_0 + a_1 R^{\Upsilon}, \tag{18}$$

with the thermal hysteresis exponent $\Upsilon = 2/3$ for sufficiently small R similar to Eq. (1), where r_0 and a_1 are constants. It is found that, the smaller the R values are, the closer Υ is to 2/3, as shown in Fig. 1(a). Similarly, the transition order parameter M_t at $r = r_{s0}$ obeys

$$M_t = M_0 + a_2 R^{\Upsilon_m}, \tag{19}$$

with the order-parameter hysteresis exponent $\Upsilon_m = 1/3$ for sufficiently small R, as shown in Fig. 1(b). One sees there that r_0 and M_0 are r_{s0} and M_{s0}, respectively.

One can also represent the transition by a susceptibility dM/dr, which exhibits a valley. The dependence of the position of its nadir, r_v, on R is depicted in Fig. 2(a). We find that r_v also follows Eq. (18) with again $\Upsilon = 2/3$ and $r_0 = r_{s0}$ for small rates. However, for the order parameter at r_v, i.e., M_v, the slopes are not 1/3, as seen in Fig. 2(b), and can be even close to 1 for vanishingly small rates.

The reason that we called this Thermal Class I a field-like class can be seen from Eq. (8). For sufficiently small R and thus τ, m is negligible. As a result, the dominant driving force is the effective field K that is equivalent to the field in the field-driven case [10, 11]. From the view of Eq. (12), a small value of R means a small τ and thus the first linear term is dominant and the second quadratic term can be ignored in Eq. (13). Consequently, a linearly varying τ is equivalent to a linearly varying K, which is just the field that drives the transition.

In this limit, Eq. (8) in the absence of the gradient term can be solved analytically as it is a kind of Riccati

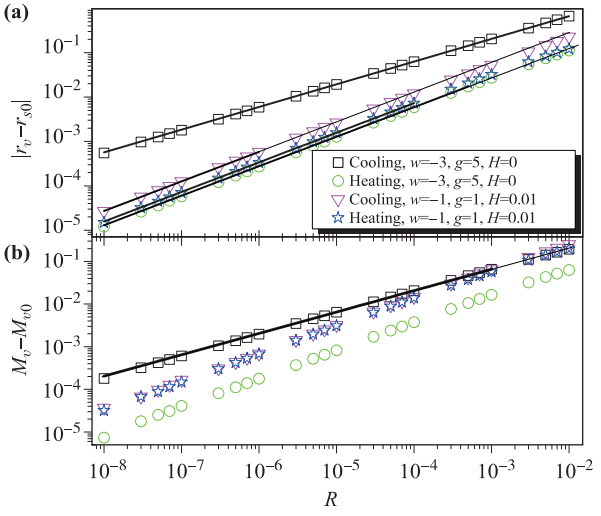

Fig. 2 Dependence of **(a)** the temperature r_v and **(b)** the order parameter M_v at the nadir of the valley of $\mathrm{d}M/\mathrm{d}r$ on the temperature sweep rate R. The thick lines are power-law fits to the data covered and the thin lines are their direct extensions. The fitted lines have slopes 0.5114(2), 0.6648(7), 0.6669(6), 0.6657(6) in (a) from up to down and 0.501(1) in (b). We use the theoretic values of r_{s0} and M_{v0} as they equal almost the corresponding values obtained by fitting the raw data instead of the subtracted ones. Data from cooling at $H = 0$ are obtained by cooling from $r = 0$ with an initial order parameter of 10^{-10}. It is found that the smaller the initial order parameter is, the closer the slopes are to the theoretical values.

equation [43]. The result is [11, 44]

$$m(t) = -\sqrt[3]{\frac{4M_{s0}R}{v^2\lambda}}\frac{c_1 Ai'\left(-\sqrt[3]{cR}t\right) + c_2 Bi'\left(-\sqrt[3]{cR}t\right)}{c_1 Ai\left(-\sqrt[3]{cR}t\right) + c_2 Bi\left(-\sqrt[3]{cR}t\right)}, \tag{20}$$

where Ai and Bi are the Airy functions, $c \equiv v\lambda^2 M_{s0}/2$, c_1 and c_2 are constants to be determined by initial conditions, and a prime indicates a derivative with respect to the argument in this subsection. Therefore, one recovers Eq. (18) with $a_1 = x_t/\sqrt[3]{g\lambda^2/2}$ and $r_0 = r_{s0}$ from Eq. (20) at $\sqrt[3]{v\lambda^2 R/2}t = x_t$ at which $m = 0$ and Eq. (19) with $a_2 = \sqrt[3]{4/g^2\lambda}[c_1 Ai'(0) + c_2 Bi'(0)]/[c_1 Ai(0) + c_2 Bi(0)]$ and $M_0 = M_{s0}$ from Eq. (20) at $K = Rt = 0$.

From Fig. 2, one sees that, although the valley temperature r_v converges to r_{s0} when $R \to 0$ as r_t does, M_v does not tend to M_{s0} but instead to M_{v0} in the same limit, which is given by

$$M_{v0} = M_{s0} - 2v/g. \tag{21}$$

This can be seen as follows.

We first notice that r_v can only approach r_{s0} for $R \to 0$. This can be inferred from the inset of Fig. 1. As

$R \to 0$, the transition between the two phases tends to r_{s0}. When $R = 0$, the transition takes place vertically at r_{s0}. Accordingly, the valleys of $\mathrm{d}M/\mathrm{d}r$ approach r_{s0} too. Also, dM/dr itself diverges there. From Eq. (8) with the neglected cubic term reinstated, one finds at the nadir of the valley

$$\frac{\mathrm{d}m}{\mathrm{d}r} = -\frac{m_v + M_{s0}}{\tau + vm_v + gm_v^2/2}, \tag{22}$$

which means either $m_{v0} = 0$ or $m_{v0} = -2v/g$ at $R = 0$ at which $\tau = 0$ and $\mathrm{d}M/\mathrm{d}r = \infty$ but with m_v finite. By Eq. (7), the solution $m_{v0} = 0$ corresponds to $M = M_{s0}$ and $m_{v0} = -2v/g$ corresponds to Eq. (21).

As M_v approaches M_{v0} at $R = 0$, we can expand M at M_{v0}, i.e., $M = M_{v0} + \overline{m}$, resulting in

$$\frac{\partial \overline{m}}{\partial t} = -\lambda\left(\tau\overline{m} - \nabla^2\overline{m} - \frac{1}{2!}v\overline{m}^2 - K + K_0\right), \tag{23}$$

from Eq. (5), where $K_0 \equiv 2v^3/(3g^2)$. The differences between Eq. (23) and Eq. (8) are only the new constant K_0 term and the opposite sign of the quadratic term. It is this opposite sign that renders $M > M_{v0}$ for both heating and cooling. The solution of Eq. (23) is again Eq. (20), only with $-t$ replaced by $t + K_0/(M_{s0}R)$. This might be argued to be a shift of r_{s0} to $r_{s0} - K_0/M_{s0}$. However, as pointed out above, r_v converges to r_{s0} instead of this shifted value.

We can now explain the results for small rates in Fig. 2. On the one hand, as r_v converges to r_{s0}, we must use Eqs. (8) and (20). The nadir of the valley must appear at a certain x_v instead of x_t at the transition temperature. This then results again in $\Upsilon = 2/3$ for small rates. On the other hand, we may directly use Eq. (23) for M_v, but now the argument of the Airy functions becomes $x_v + (K_0\sqrt[3]{c}/M_{s0})R^{-2/3}$, which is strongly R dependent for small R. Accordingly, M_v is not just controlled by the prefactor $R^{1/3}$.

3.2.2 Thermal Classes II and III

Detailed analysis, however, reveals that there is another class with a different Υ. This can be readily seen from the cooling transition taking place at $H = 0$. In this case, the instability point is $(r_{s0}^-, M_{s0}^-) = (0, 0)$. As mentioned above, Eq. (8) and Eq. (5) are then identical up to the quadratic term. Because the transition is at $r = 0$, the leading term of the free energy is again ϕ^3 and ought to be described by a ϕ^3 theory too. Indeed, one finds that, in this case, r_v and M_v follow Eqs. (18) and (19) with Υ and Υ_m, now denoted as $\ddot{\Upsilon}$ and $\ddot{\Upsilon}_m$, respectively, for Thermal Class III, of $\sim$1/2, being distinct from the above case, as can be seen from Fig. 2. Accordingly, it is important to use Eq. (18) instead of Eq. (1) to correctly identify the scaling, at least in this special case in which the heating and cooling transitions behave distinctly.

In fact, similar to the purely thermal class of the cooling transition at $H = 0$, there exist other cases in which the hysteresis exponents are close to 1/2. Figure 2 demonstrates that, for a range of large R values, Υ and Υ_m are also close to 1/2. Moreover, even in the heating transition, they can also be close to 1/2, as Fig. 2 indicates. We classify these as Thermal Class II and denote its Υ and Υ_m with an overdot. In Fig. 1(a), the slopes for r_t also decrease for large R. However, M_t appears to be saturated at high rates. Although, in the mean field, the hysteresis exponents of this class are identical with those of Thermal Class III, the above results indicate that this class emerges when τm instead of K dominates. In other words, it is described by Eq. (14) with a linearly varying $\overline{\tau}$ since the second term in Eq. (15) can be ignored for large τ. As it can cross over to the field-like class (see below), we also call Thermal Class II a partly thermal class to distinguish it from the purely thermal class.

Indeed, when K is omitted, Eq. (8) in the absence of the gradient term becomes a Bernoulli's equation that is solved by [43]

$$m = \frac{\sqrt{R}\exp\left\{-\frac{1}{2}\lambda\left[\left(\frac{\tau}{\sqrt{R}}\right)^2 - \left(\frac{\tau_0}{\sqrt{R}}\right)^2\right]\right\}}{\sqrt{R}m_0 + \frac{1}{2}\lambda v\int_{\tau_0/\sqrt{R}}^{\tau/\sqrt{R}}\exp\left[-\frac{1}{2}\lambda(\tau'^2 - \tau_0^2/R)\right]\mathrm{d}\tau'}, \tag{24}$$

where $m(\tau_0) \equiv m_0$ and the integral can be expressed as error functions. One sees that τ appears in the solution through the combination $\tau/\sqrt{R}$. Consequently, at certain loci of certain functions of the solution, τ is expected to be proportional to $R^{1/2}$ though with possible corrections from the initial condition.

3.2.3 Crossover between Thermal Classes I and II

We have seen that, except for cooling in the absence of an external field, a situation that leads to the purely thermal class (III), in the presence of an external field, there exist two thermal classes (I and II) that exhibit different behaviors for large and small rates, respectively.

In the median range of R between the two extremal cases, one finds from Fig. 2 that Υ falls between 2/3 and 1/2. This stems from the nonlinearity of $\overline{K}$ and $\overline{\tau}$ and reflects the competition between their two components in Eqs. (13) and (15), respectively.

Owing to this crossover, only sufficiently small R can give rise to $\Upsilon = 2/3$. However, it was found numerically and even experimentally [9] that the exponent of the thermal hysteresis areas in the M^2–r frame is still close to 2/3 for not-so-large R. The area in the M–r frame is

$$A = \oint M\mathrm{d}r = \int_{r_{\mathrm{down}}}^{r_{\mathrm{up}}}(M_+ - M_-)\mathrm{d}r$$

$$\simeq \left(\int_{r_v^-}^{r_{s0}^-} + \int_{r_{s0}^-}^{r_{s0}^+} + \int_{r_{s0}^+}^{r_v^+}\right)(M_{s0}^+ + m_+ - M_{s0}^- - m_-)\mathrm{d}r$$
$$\sim A_0 + \left(M_{s0}^+ - M_{s0}^-\right)\left(a_1^+ R^{\Upsilon^+} + a_1^- R^{\Upsilon^-}\right) \quad (25)$$

to the leading order in R, where $+$ $(-)$ denotes variables in heating (cooling), $r_{\rm down}$ $(r_{\rm up})$ denotes the lowest (highest) temperature delimitating the hysteresis loop, $A_0 = \int_{r_{s0}^-}^{r_{s0}^+}(M_+ - M_-)\mathrm{d}r$ at equilibrium, and Eqs. (7) and (18) have been used. We have neglected the contributions from Eq. (19) since $m_t = M_t - M_{s0}$ is negligible, as can be seen from the inset of Fig. 1. Indeed, we could not detect this leading order in R for very small R. Note that we have employed r_v for r but M_t for M, as r_v extends beyond r_t in both heating and cooling and may provide a better approximation than the latter does but M_v does not converge to M_{s0}. A similar approximate expression can be written for the area in the M^2–r frame, which is proportional to the energy dissipation. We see that both areas show similar behavior in the approximations embodied in Eq. (25). However, the exponent found from the M^2–r frame is always larger than that from the M–r frame regardless of whether M_{s0} is large or small. One possible reason for this is that the approximation near the heating spinodal is always better in the former frame regardless of whether M_{s0} is large or small, while the approximation near the cooling spinodal is always poor and may obscure the behavior there, as can also been seen from the inset of Fig. 1. Comparing Fig. 1(a) with Fig. 2(a), one finds that the fitted ranges of R are wider and the slopes are larger for r_v than those for r_t in heating. This may indicate that the area may have even favorable results and may thus be another reason for the larger exponent in the M^2–r frame.

4 Scaling theory

To relate the hysteresis exponents Υ and Υ_m to more fundamental exponents, we now perform a scaling analysis for the models.

4.1 General scaling forms

First, we consider the massless theory (12). Following [10], we perform a scale transformation to it by reducing the length scale by ρ, i.e., $|\boldsymbol{r}'| = |\boldsymbol{r}|/\rho$. Then,

$$\nabla'^2 = \rho^2\nabla^2, \quad (\lambda t)' = (\lambda t)\rho^{-z}, \quad \varphi' = \varphi\rho^{\beta/\nu},$$
$$\overline{K}' = \overline{K}\rho^{\beta\delta/\nu}, \quad v' = v\rho^y, \quad \tau' = \tau\rho^{1/\nu}, \quad (26)$$

where β, ν, δ, and z are the instability exponents corresponding to the standard critical exponents and y is a constant. We have set λ as the unit of time t as usual [10]. Note that M_{s0} changes also like φ. Invariance of Eqs. (12) and (13) under this transformation leads to $z = 1/\nu = 2$, $\beta(\delta - 1) = 1$, $y = (1 - \beta)/\nu$, and

$$\varphi(t, \overline{K}) = \rho^{-\beta/\nu}\varphi(t\rho^{-z}, \overline{K}\rho^{\beta\delta/\nu}), \quad (27)$$

or

$$\varphi(t, \overline{K}) = t^{-\beta/(\nu z)} f_K(\overline{K} t^{\beta\delta/(\nu z)}), \quad (28)$$

by choosing a scale ρ such that $t\rho^{-z}$ becomes a constant, where f_K is a scaling function. We have neglected dimensional factors for simplicity.

Note that we can also obtain the scaling laws among the exponents from the invariance of Eq. (8). The only problem with this dynamic equation is the redundancy of the parameters.

We have suppressed the coupling v in Eqs. (27) and (28). In fact, for a renormalizable theory [45–48], v should be dimensionless and thus should remain invariant. This dictates $y = 0$ or $\beta = 1$ and hence $\delta = 2$. In addition, the susceptibility exponent $\gamma = \beta(\delta - 1) = 1$. The scaling laws $\gamma/\nu = 2 - \eta$ and $\alpha + 2\beta + \gamma = 2$ then lead to $\eta = 0$ and $\alpha = -1$, which in turn results in an upper critical dimension $d_c = 6$ owing to the hyperscaling law $\alpha = 2 - d\nu$, in agreement with the dimensional analysis [10, 11]. These complete the list of the usual mean-field instability exponents. They all share identical meaning with their critical counterparts [10, 11].

Equation (28) can be written in an FTS form in terms of the rate R. In linearly temperature-driven FOPTs, $\tau = r - r_{s0} = Rt$. Using Eq. (13), we obtain

$$\varphi = (\tau/R)^{-\frac{\beta}{\nu z}} f_K\left[\left(\tau^{\frac{2\nu z+\beta\delta}{\nu z}}/(2v) - M_{s0}\tau^{\frac{\beta\delta+\nu z}{\nu z}}\right)R^{-\frac{\beta\delta}{\nu z}}\right]. \quad (29)$$

Therefore, from Eq. (10),

$$m(\tau, R) = -\tau/v + (\tau/R)^{-\frac{\beta}{\nu z}} \times f_K\left[\left(\tau^{\frac{2\nu z+\beta\delta}{\nu z}}/(2v) - M_{s0}\tau^{\frac{\beta\delta+\nu z}{\nu z}}\right)R^{-\frac{\beta\delta}{\nu z}}\right]. \quad (30)$$

For the purely massive theory (14), although $\overline{\tau}$ is like τ, we assume that it may scale distinctly from the latter with an exponent $\overline{\nu}$. Therefore,

$$\varphi(t, \overline{\tau}) = \rho^{-\beta/\nu}\varphi(t\rho^{-z}, \overline{\tau}\rho^{1/\overline{\nu}}). \quad (31)$$

Then, a similar method leads to

$$m(\tau, R) = (\tau/R)^{-\frac{\beta}{\nu z}} f_{\overline{\tau}}\left[\left(\tau^{\frac{2\overline{\nu}z+2}{\overline{\nu}z}} - 2vM_{s0}\tau^{\frac{\overline{\nu}z+2}{\overline{\nu}z}}\right)R^{-\frac{2}{\overline{\nu}z}}\right] - \tau/v - \sqrt{\tau^2 - 2vM_{s0}\tau}/v \quad (32)$$

using Eqs. (10) and (15), where $f_{\overline{\tau}}$ is another scaling function.

Of course, for the purely thermal class, $M_{s0}=0$ and $\overline{\tau}$ is just τ. Therefore, the scaling form (32) simplifies to

$$M(\tau,R)=(\tau/R)^{-\frac{\beta}{\nu z}}f_\tau\left(\tau^{\frac{1+\nu z}{\nu z}}R^{-\frac{1}{\nu z}}\right), \tag{33}$$

or to a standard FTS form

$$M(\tau,R)=R^{\frac{\beta}{1+\nu z}}f_{\tau 1}\left(\tau R^{-\frac{1}{1+\nu z}}\right), \tag{34}$$

where f_τ is yet another scaling function and $f_{\tau 1}(x)=x^{-\beta/(\nu z)}f_\tau(x^{1+1/(\nu z)})$.

In the mean field, the value of $\overline{\nu}$ is identical to that of ν. However, we shall see that they are different in value in the non-mean-field case.

4.2 Limiting cases and their thermal hysteresis exponents

Equations (30) and (32) are equivalent general descriptions of the scaling behavior in the vicinity of the instability points of the temperature-driven FOPTs. Because they are quite complicated owing to the nonlinearity of $\overline{K}$ and $\overline{\tau}$, the thermal hysteresis exponents cannot be read out directly. Note that, if one varied $\overline{K}$ and $\overline{\tau}$ instead of τ itself linearly, a simple FTS form would be present, similar to Eq. (33). Further, the two parameters $\overline{K}$ and $\overline{\tau}$, in fact, contain only one independent combination, $\tau^2-2vM_{s0}\tau$. Therefore, simple scaling forms would be obtained by varying this factor linearly. However, simple scaling forms do appear and the hysteresis exponents can be readily identified in the two limits in which either the linear or the quadratic term alone in $\overline{K}$ and $\overline{\tau}$ is kept. This results in the field-like universality class and the partly thermal class, respectively. In contrast, the scaling form (33) or (34) gives rise to the purely thermal class.

4.2.1 Thermal Class I

The field-like universality class can be obtained from either Eq. (30) or (32). We start with the massless theory, Eq. (30).

When the term linear in τ in $\overline{K}$ dominates owing to R being small, we omit the quadratic term in Eq. (30) and obtain

$$m(\tau,R)=R^{\frac{\beta}{\beta\delta+\nu z}}f_{K1}\left(\tau R^{-\frac{\beta\delta}{\beta\delta+\nu z}}\right)-\tau/v \tag{35}$$

with $f_{K1}(x)=x^{-\beta/(\nu z)}f_K[-M_{s0}x^{(\beta\delta+\nu z)/(\nu z)}]$.

From Eq. (35), thermal hysteresis exponents can be obtained. Indeed, for $\tau=0$ or $r=r_{s0}$, Eq. (35) results in Eq. (19) with

$$\Upsilon_m=\frac{\beta}{\beta\delta+\nu z}, \tag{36}$$

$M_{s0}=M_0$, and $a_2=f_{K1}(0)$ by using Eq. (7). For $M=M_{s0}$ or $m=0$ for which $\tau=\tau_t$, we have

$$f_{K1}\left(\tau_t R^{-\frac{\beta\delta}{\beta\delta+\nu z}}\right)=\tau_t R^{\frac{-\beta}{\beta\delta+\nu z}}/v. \tag{37}$$

Since $\delta>1$, the argument on the left dominates, so

$$\tau_t=r_t-r_{s0}=R^{\Upsilon}f_{K2}(R^{\Upsilon-\Upsilon_m}), \tag{38}$$

where $f_{K2}^{-1}(x)=vf_{K1}(x)/x$,

$$\Upsilon=\frac{\beta\delta}{\beta\delta+\nu z}, \tag{39}$$

and $r_0=r_{s0}$ from Eqs. (18) and (9a). Note that $\Upsilon-\Upsilon_m=\gamma/(\beta\delta+\nu z)>0$ and thus $f_{K2}(x)$ constitutes a proper correction to the leading scaling [49].

In contrast, from the scaling form of the purely massive theory, Eq. (32), keeping only the leading τ term, we have

$$m(\tau,R)=R^{\frac{\beta\overline{\nu}}{(2+\overline{\nu}z)\nu}}f_{\overline{\tau}1}\left(\tau R^{-\frac{2}{2+\overline{\nu}z}}\right)+\sqrt{-2M_{s0}\tau/v} \tag{40}$$

with $f_{\overline{\tau}1}(x)=x^{-\beta/(\nu z)}f_{\overline{\tau}}[-2vM_{s0}x^{(2+\overline{\nu}z)/(\overline{\nu}z)}]$. Therefore, for $\tau=0$, we again arrive at Eq. (19) but with

$$\Upsilon_m=\frac{\beta\overline{\nu}}{(2+\overline{\nu}z)\nu} \tag{41}$$

and $a_2=f_{\overline{\tau}1}(0)$ now. For $m=0$, we write

$$\tau_t=r_t-r_{s0}=R^{\Upsilon}f_{\overline{\tau}2}(R^{\Upsilon/2-\Upsilon_m}) \tag{42}$$

with

$$\Upsilon=\frac{2}{2+\overline{\nu}z}, \tag{43}$$

where $f_{\overline{\tau}2}^{-1}(x)=\sqrt{-v/(2M_{s0})}f_{\overline{\tau}1}(x)/\sqrt{x}$. In this case, however, since $\beta=1$, $\Upsilon/2-\Upsilon_m=0$; thus, the correction $f_{\tau 2}$ in Eq. (42) is just a constant.

In the mean field, we have $\overline{\nu}z=1$ and $\beta\delta=2$. Consequently, both Eqs. (36) and (41) and both Eqs. (39) and (43) yield $\Upsilon_m=1/3$ and $\Upsilon=2/3$, respectively, consistently in agreement with numerical results, though, as mentioned, the purely massive theory may be real only in the cooling transitions in the absence of an external field.

We have shown that the two reduced theories are indeed equivalent in the mean field. In fact, since we consider essentially the effective field K in this class and ignore the mass term, we can only study the massless theory with K replacing $\overline{K}$ directly. This has been studied previously [10, 11] and yields, of course, identical exponents, albeit without the correction f_{K2}.

In the case of $\overline{m}$ in Eq. (23), K_0 acts as a relevant constant external field. Accordingly, the scaling function, f_{K1} for example, has $K_0R^{-\beta\delta/(\beta\delta+\nu z)}$ as its additional argument. This destroys the simple scaling and is consistent with the mean-field theory and Fig. 2(b).

4.2.2 Thermal Class II

In this case, we keep only the quadratic terms in $\overline{K}$ and $\overline{\tau}$. This means that we neglect the effective field K and hence $\overline{\tau}$ is just τ and φ is just m. Accordingly, for the purely massive theory, Eq. (32) becomes

$$m(\tau,R)=R^{\frac{\beta\overline{\nu}}{(1+\overline{\nu}z)\nu}}f_{\overline{\tau}3}\left(\tau R^{-\frac{1}{1+\overline{\nu}z}}\right) \tag{44}$$

with $f_{\overline{\tau}3}(x)=x^{-\beta/(\nu z)}f_{\overline{\tau}}[x^{(2+2\overline{\nu}z)/(\overline{\nu}z)}]$. Thus, one readily obtains

$$\dot{\Upsilon}_m=\frac{\beta\overline{\nu}}{(1+\overline{\nu}z)\nu},\quad \dot{\Upsilon}=\frac{1}{1+\overline{\nu}z}. \tag{45}$$

The scaling form of the massless theory, Eq. (30), can also lead to this class, of course. It becomes

$$m(\tau,R)=R^{\dot{\Upsilon}_m}f_{K3}\left(\tau R^{-\dot{\Upsilon}}\right)-\tau/v \tag{46}$$

with $f_{K3}(x)=x^{-\beta/(\nu z)}f_K[x^{(\beta\delta+2\nu z)/(\nu z)}/v]$ and

$$\dot{\Upsilon}_m=\frac{2\beta}{\beta\delta+2\nu z},\quad \dot{\Upsilon}=\frac{\beta\delta}{\beta\delta+2\nu z} \tag{47}$$

in the same limit. However, there is a subtlety here. In the mean-field approximation, $\delta=2$ and hence $\dot{\Upsilon}_m=\dot{\Upsilon}$ and no correction is necessary. If $d<d_c$, $\delta<2$ [11] and hence $\dot{\Upsilon}_m>\dot{\Upsilon}$. The argument from Eq. (37) to (38) then gives rise to a surprising consequence: Both the temperature hysteresis exponent and the order-parameter hysteresis exponent equal $\dot{\Upsilon}_m$ and the correction exponent is $\dot{\Upsilon}_m-\dot{\Upsilon}>0$.

In the mean field, both theories again yield the same exponents of $\dot{\Upsilon}_m=1/2=\dot{\Upsilon}$, in agreement with numerical results shown in Fig. 2.

4.2.3 Thermal Class III

With similar procedures, we can obtain directly the hysteresis exponents for this purely thermal class as

$$\ddot{\Upsilon}_m=\frac{\beta}{1+\nu z},\quad \ddot{\Upsilon}=\frac{1}{1+\nu z}, \tag{48}$$

using the scaling form (34). In the mean-field approximation, $\overline{\nu}=\nu$ and thus Eq. (48) is just Eq. (45).

4.3 General purely thermal class

We mentioned in Section 2 that the cooling transition of a ϕ^6 model at $H=0$ falls into a different class. In this section, we study briefly this issue.

Consider the general model (17) with an external field H. Although, in this class, $H=0$, we retain H to gather sufficient information. A scaling transformation similar to Eq. (26) with $y=0$ then leads to $z=1/\nu=2$ and $\beta=1/(\sigma-1)$. Combining this with the scaling laws mentioned in Section 4.1, we find then $\gamma=1$, $\delta=\sigma$, $\eta=0$, $\alpha=(\sigma-3)/(\sigma-1)$, and the upper critical dimension $d_c=2(\sigma+1)/(\sigma-1)$. This d_c conforms again with the naive dimensional analysis. Therefore, from Eq. (48), we see that, in this case, although the value of $\ddot{\Upsilon}$ is identical to the value obtained from model (2), that of $\ddot{\Upsilon}_m$ may be different.

For the ϕ^6 model, $\sigma=3$. Therefore, we have $\beta=1/2$, $d_c=4$, and so on, though $z=1/\nu=2$. In fact, this is just the usual ϕ^4 model for the critical phenomena of the Ising universality class. The hysteresis exponents for this class have already been computed in Ref. [40]. They are different from those of the thermal transitions of the ϕ^3 model studied here, which has $\sigma=2$. However, we still classify both models into Thermal Class III as both are concerned with the cooling transition in the absence of the external field.

5 Renormalization group theory

Our task is to confirm the scaling for $d<d_c$ and to calculate the scaling exponents. This can be done by using an RG analysis [45–48, 50, 51]. An RG study of the dynamics of the full ϕ^3 theory (8) with Gaussian white noise (4) for the Yang–Lee edge singularity has been presented in Ref. [39] using shift invariance. A detailed RG study of the massless theory (12) has been performed in [11] with hysteresis exponents for the field-driven FOPTs computed in three- and two-loop orders for the static and dynamic exponents, respectively. Accordingly, we may just insert those exponents for the relevant classes. In fact, the exponents for the field-like class are just identical to those of the field-driven FOPTs. Because the massless and massive theories are equivalent, comparing Eqs. (36) and (39) with Eqs. (41) and (43) and Eq. (45) with (47), one sees that, for both pairs of exponents to be identical, one must have surprisingly $\overline{\nu}=2\nu/(\beta\delta)$, the values of which are indeed equal in the mean field. We shall study RG theory to prove this and to prove the equivalence of the two theories.

5.1 Fluctuation shifts and relationship between temperature and field

We start with the full dynamic model (2) with Gaussian white noise (4). It is well established that it can be recast into a field-theoretic form with a dynamic functional [45, 48, 52–54],

$$I[\phi,\widetilde{\phi}]=\int \mathrm{d}\boldsymbol{x}\mathrm{d}t\left\{\widetilde{\phi}\left[\frac{\partial\phi}{\partial t}+\lambda(r-\nabla^2)\phi+\frac{1}{2!}\lambda w\phi^2+\frac{1}{3!}\lambda g\phi^3-\lambda H\right]-\lambda\widetilde{\phi}^2\right\}, \tag{49}$$

by introducing an auxiliary response field $\widetilde{\phi}$ [55]. Then, the generating functionals for connected and vertex response and correlation functions can be defined and perturbation expansions using Feynman diagrams can be set up.

Assuming that the instability point is now at (r_s, M_s) and $\widetilde{\phi} = 0$, we expand at M_s but near r_s for a constant uniform field H by setting

$$\phi = M_s + \varphi, \quad \widetilde{\phi} = \widetilde{\varphi}, \tag{50}$$

and we neglect again the cubic term. Equation (49) then changes into

$$I[\varphi,\widetilde{\varphi}] = \int \mathrm{d}\boldsymbol{x}\mathrm{d}t \left\{ \widetilde{\varphi}\left[\frac{\partial\varphi}{\partial t} + \lambda(\tau - \nabla^2)\varphi + \frac{1}{2!}\lambda v\varphi^2 - \lambda K\right] - \lambda\widetilde{\varphi}^2 \right\}, \tag{51}$$

with

$$\tau = r + wM_s + \frac{1}{2}gM_s^2, \tag{52a}$$

$$K = H - rM_s - \frac{1}{2}wM_s^2 - \frac{1}{3!}gM_s^3, \tag{52b}$$

$$v = w + gM_s, \tag{52c}$$

similar to Eq. (9). In the mean-field approximation, $r_s = r_{s0}$ and $M_s = M_{s0}$ and thus we recover Eq. (9). When fluctuations are taken into account, the instability point now shifts from $\tau_{s0} = K_{s0} = 0$ to $\tau = \tau_s$ and $K = K_s$ determined by [10, 11]

$$\Gamma^{(11)}(\boldsymbol{0}, 0) = 0, \tag{53a}$$

$$\langle\varphi\rangle = 0 \quad \text{or} \quad \Gamma^{(10)}(\boldsymbol{0}, 0) = \lambda K_s, \tag{53b}$$

i.e.,

$$\tau_s = \frac{1}{2}v^2 \int \frac{\mathrm{d}\boldsymbol{k}}{(2\pi)^d} \frac{1}{(\boldsymbol{k}^2 + \tau_s)^2}, \tag{54a}$$

$$K_s = \frac{1}{2}v \int \frac{\mathrm{d}\boldsymbol{k}}{(2\pi)^d} \frac{1}{\boldsymbol{k}^2 + \tau_s}, \tag{54b}$$

to one-loop order, or

$$\tau_s^{3-d/2} = \frac{\Gamma(3-d/2)\Gamma(d/2)}{2(4-d)} v^2 N_d, \tag{55a}$$

$$K_s = \frac{\Gamma(3-d/2)\Gamma(d/2)}{(2-d)(4-d)} v N_d \tau_s^{d/2-1}, \tag{55b}$$

where $\Gamma^{(\widetilde{N}N)}$ is the vertex function, $N_d = 2/[(4\pi)^{d/2}\Gamma(d/2)]$ (where Γ is the Euler gamma function), the angle brackets denote the average over the action, and $\{\boldsymbol{q}, \omega\}$ represents a set of momenta and frequencies. Similar to the theory of critical phenomena [45–48], Eq. (53a) implies the divergence of the inverse susceptibility at the instability point. Divergences of the correlation function at long distances and the correlation length at the instability point can also be derived within the theory. However, the real correlation length of the original FOPT does not diverge because of the irrelevant higher order terms. Equation (55) satisfies the relation

$$K_s + \tau_s^2/(2v) = 0 \tag{56}$$

near $d = 6$. Using τ_s and K_s, which satisfy Eq. (52) at r_s, we can rewrite the first two equations in Eq. (52) as

$$\tau - \tau_s = r - r_s, \tag{57a}$$

$$K - K_s = -M_s(r - r_s) = -M_s(\tau - \tau_s). \tag{57b}$$

This indicates that the relation between τ and K for temperature-driven FOPTs is still valid after the shifts even if the fluctuations are taken into account.

One sees that the cooling instability point in the absence of an external field now has generally $M_s \neq 0$ because K_s is finite for a φ^3 theory. This is qualitatively different from a φ^4 $\sigma = 3$ theory, in which the symmetry forbids a K_s term. Therefore, although in the mean field we have Thermal Class III described by the purely thermal model, it is removed by fluctuations. However, it survives in the generalized purely thermal model with an odd σ.

5.2 Renormalization factors and their relations

After the mass and field renormalizations, the theory becomes massless at the instability point. Consequently, its perturbation expansions are plagued with infrared divergences. Yet, it turns out that these divergences can be removed by renormalization factors Z defined as [39, 48]

$$\begin{aligned}
&\varphi = Z_\varphi^{1/2}\varphi_R, \quad \widetilde{\varphi} = Z_{\widetilde{\varphi}}^{1/2}\widetilde{\varphi}_R, \quad \tau - \tau_s = Z_\varphi^{-1}Z_\tau\tau_R,\\
&\lambda = Z_\lambda\lambda_R = (Z_\varphi/Z_{\widetilde{\varphi}})^{1/2}\lambda_R, \quad u = vN_d^{1/2}\mu^{-\epsilon/2},\\
&u = Z_\varphi^{-3/2}Z_v u_R, \quad v = Z_\varphi^{-3/2}Z_v v_R,\\
&K - K_s = Z_\varphi^{-1/2}[K_R + Z_0\tau_R^2/(2v_R)],
\end{aligned} \tag{58}$$

such that the renormalized vertex function

$$\Gamma_R^{(\widetilde{N}N)}(\{\boldsymbol{q}, \omega\}) = (Z_{\widetilde{\varphi}}^{\widetilde{N}/2}/Z_\varphi^{N/2})\Gamma^{(\widetilde{N}N)}(\{\boldsymbol{q}, \omega\}) \tag{59}$$

[for $(\widetilde{N}, N) \neq (1, 0)$] in terms of the renormalized functions becomes finite, since the dimensional poles at $\epsilon = 6 - d \to 0$ have then been subtracted and just subtracted in the minimal RG scheme with dimensional regulation [56], where the subscripts R denote renormalized variables and μ is an arbitrary momentum scale. This RG

method has an additional advantage of decoupling statics from dynamics [57] so that the static renormalization factors can be chosen as the equilibrium ones.

The renormalization factors are, however, not all independent. The shift symmetry of Eq. (51) with respect to the shift of the order parameter gives rise to some exact relations among them [39, 48].

For an arbitrary shift of $\varphi' = \varphi + c$, owing to invariance [39, 48], the shifted variables, Eq. (11), ought to share the same relations and renormalization factors as the original ones. Therefore,

$$\varphi' = Z_\varphi^{1/2}\varphi'_R = \varphi + c = Z_\varphi^{1/2}\varphi_R + Z_c c_R, \tag{60}$$

which means $Z_c = Z_\varphi^{1/2}$ since $Z_\varphi^{-1/2}Z_c$ is a finite quantity that in the minimal renormalization reduces to unity. Applying this result with Eq. (58) to Eq. (11a), we have

$$\begin{aligned}\tau' &= Z_\varphi^{-1}Z_\tau\tau'_R + \tau_s = \tau - vc \\ &= Z_\varphi^{-1}Z_\tau\tau_R - Z_\varphi^{-1}Z_v v_R c_R + \tau_s,\end{aligned} \tag{61}$$

which leads to $Z_\tau = Z_v$. Similarly, from Eqs. (58) and (11b) we get

$$K'_R = K_R + (Z_0 + Z_\tau)\left(\tau_R c_R - \frac{1}{2}v_R c_R^2\right). \tag{62}$$

Therefore, we have

$$Z_\tau = Z_v = 1 - Z_0. \tag{63}$$

This result indicates that, among the four static renormalization factors introduced in Eq. (58), only two are independent. The Z factor for the vertex will be chosen to determine the fixed point and the other one will determine the only independent static exponent. The two other factors, Z_λ and $Z_{\widetilde{\varphi}}$, which are related by the fluctuation-dissipation theorem [45, 48, 52–54] to ensure a correct static limit [11], determine one independent dynamic exponent.

Equation (63) can also be obtained from Ward's identities stemming from the continuous shift symmetry [39]. Taking the derivative of the shifted vertex functions with respect to c at $c = 0$ results in Ref. [39]

$$\begin{aligned}\Gamma_R^{(\widetilde{N}N+1)}(\{\boldsymbol{q},\omega\},\tau_R) =& Z_v Z_\tau^{-1} v_R \frac{\partial}{\partial\tau_R}\Gamma_R^{(\widetilde{N}N)}(\{\boldsymbol{q},\omega\},\tau_R) \\ &+ \left(Z_\tau + Z_0 Z_v Z_\tau^{-1}\right)\tau_R\delta_{N1},\end{aligned} \tag{64}$$

where δ_{N1} is the Kronecker delta function. Equation (64) leads to Eq. (63) since the renormalized vertex functions possess no poles and the combinations of the Z factors must be finite.

To one-loop order, it is readily found [10, 11] that

$$Z_\varphi = 1 - u_R^2/(6\epsilon), \quad Z_v = 1 - u_R^2/\epsilon, \quad Z_{\widetilde{\varphi}} = 1 - u_R^2/(3\epsilon). \tag{65}$$

These static and dynamic factors have been found to three-loop order [58, 59] and two-loop order [39], respectively.

It is instructive to know the renormalization of $\overline{K}$ and $\overline{\tau}$, which are K' and τ' at some particular c. From Eqs. (13), (15), (58), and (63), we find

$$\begin{aligned}\overline{K} &= (K - K_s) + (\tau - \tau_s)^2/(2v) \\ &= Z_\varphi^{-1/2}\left[K_R + \tau_R^2/(2v_R)\right] = Z_\varphi^{-1/2}\overline{K}_R,\end{aligned} \tag{66}$$

$$\begin{aligned}\overline{\tau}^2 &= (\tau - \tau_s)^2 + 2v(K - K_s) \\ &= Z_\varphi^{-2}Z_v\left(\tau_R^2 + 2v_R K_R\right) = Z_\varphi^{-2}Z_\tau\overline{\tau}_R^2.\end{aligned} \tag{67}$$

One notices that both $\overline{K}$ and $\overline{\tau}$ are renormalized simply, in contrast with the inhomogeneity of the renormalization of K itself. Note that $\overline{\tau}^2$ is not renormalized simply as τ^2. This underlies the difference between them.

The particular renormalization of K in Eq. (58) is to subtract divergent tadpole contributions [39, 48]. Because

$$\begin{aligned}&\Gamma^{(10)}(\{\boldsymbol{0},0\},\tau,u) = \lambda K, \\ &\Gamma_R^{(10)}(\{\boldsymbol{0},0\},\tau_R,u_R) = \lambda_R K_R,\end{aligned} \tag{68}$$

then, along with (58), we get

$$\begin{aligned}\Gamma_R^{(10)}(\{\boldsymbol{0},0\},\tau_R,u_R) = Z_{\widetilde{\varphi}}^{1/2}\Gamma^{(10)}(\{\boldsymbol{0},0\},\tau,u) \\ - Z_0\lambda_R\tau_R^2/(2v_R).\end{aligned} \tag{69}$$

Indeed, after the mass renormalization, to one-loop order, $\Gamma^{(10)} = \lambda N_d v(\tau - \tau_s)^{2-\epsilon/2}/(2\epsilon)$, which is just canceled by the subtraction in Eq. (69) to the same order.

5.3 Renormalization group equations and their solutions for the general theory

The scaling and universality behavior can be derived from an RG equation [45–48, 50, 51]. In this section, we shall study the scaling behavior of the general theory (51) to collect necessary ingredients for the reduced massless and purely massive theories in the next section. It will be seen that the solution to the RG equation automatically combines K with τ according to Eq. (13).

We first consider $\Gamma^{(1N)}$. At the instability point, $m \equiv \langle\varphi\rangle = 0$. Exploiting the independency of the bare vertex on the momentum scale μ, one finds

$$\begin{aligned}\left(\mu\frac{\partial}{\partial\mu} + \beta\frac{\partial}{\partial u_R} + \gamma_\lambda\lambda_R\frac{\partial}{\partial\lambda_R} + \overline{\gamma}_\tau\tau_R\frac{\partial}{\partial\tau_R}\right. \\ \left. -\frac{1}{2}\widetilde{\gamma} - \frac{1}{2}N\gamma\right)\Gamma_R^{(1N)} = \delta_{N0}\gamma_\tau\tau_R^2/(2v_R),\end{aligned} \tag{70}$$

from Eqs. (59) and (69), where the Wilson functions are defined as derivatives at constant bare parameters as

$$\gamma(u_R)=\mu\frac{\partial \ln Z_\varphi}{\partial\mu},\quad \overline{\gamma}_\tau(u_R)=\mu\frac{\partial \ln \tau_R}{\partial\mu}=\gamma-\gamma_\tau,\quad \gamma_\lambda(u_R)=\mu\frac{\partial \ln \lambda_R}{\partial\mu}=\frac{1}{2}\widetilde{\gamma}-\frac{1}{2}\gamma,$$
$$\widetilde{\gamma}(u_R)=\mu\frac{\partial \ln Z_{\widetilde{\varphi}}}{\partial\mu},\quad \gamma_\tau(u_R)=\mu\frac{\partial \ln Z_\tau}{\partial\mu}=\mu\frac{\partial \ln Z_v}{\partial\mu},\quad \beta(u_R)=\mu\frac{\partial u_R}{\partial\mu}=-u_R\left(\frac{1}{2}\epsilon-\frac{3}{2}\gamma+\gamma_\tau\right), \tag{71}$$

with the help of Eqs. (58) and (63). The inhomogeneous term in Eq. (70) comes from the subtraction in Eq. (69).

However, we are interested in the behavior near the instability point. For $r\neq r_c$, $m\neq 0$, the usual method is then to expand $\Gamma^{(10)}(m)$ at $m=0$, so we have

$$\lambda_R K_R(\omega,\lambda_R,\tau_R,m_R,u_R,\mu)=\Gamma_R^{(10)}(\omega,\lambda_R,\tau_R,m_R,u_R,\mu)=\sum_{N=1}^{\infty}\frac{1}{N!}\Gamma_R^{(1N)}(\omega,\lambda_R,\tau_R,0,u_R,\mu)m_R^N, \tag{72}$$

where

$$m=Z_\varphi^{1/2}m_R, \tag{73}$$

similar to φ. Using Eqs. (70) and (73), we then obtain the following inhomogeneous RG equation for K_R:

$$\left[\mu\frac{\partial}{\partial\mu}+\beta\frac{\partial}{\partial u_R}+\gamma_\lambda\lambda_R\frac{\partial}{\partial\lambda_R}+\overline{\gamma}_\tau\tau_R\frac{\partial}{\partial\tau_R}-\frac{1}{2}\gamma\left(1+m_R\frac{\partial}{\partial m_R}\right)\right]K_R(\omega,\lambda_R,\tau_R,m_R,u_R,\mu)=\gamma_\tau\tau_R^2/(2v_R). \tag{74}$$

This equation can also be obtained directly from Eq. (58) if one assumes K_R is a function of the other variables including m_R that satisfies Eq. (73).

Equation (74) is inhomogeneous. However, in terms of $\overline{K}_R$, similar to the definition in Eq. (13) and used in Eq. (66), the equation can be rewritten into the homogeneous form

$$\left[\mu\frac{\partial}{\partial\mu}+\beta\frac{\partial}{\partial u_R}+\gamma_\lambda\lambda_R\frac{\partial}{\partial\lambda_R}+\overline{\gamma}_\tau\tau_R\frac{\partial}{\partial\tau_R}-\frac{1}{2}\gamma\left(1+m_R\frac{\partial}{\partial m_R}\right)\right]\overline{K}_R(\omega,\lambda_R,\tau_R,m_R,u_R,\mu)=0 \tag{75}$$

by noting that

$$\left[\mu\frac{\partial}{\partial\mu}+\beta\frac{\partial}{\partial u_R}+\gamma_\lambda\lambda_R\frac{\partial}{\partial\lambda_R}+\overline{\gamma}_\tau\tau_R\frac{\partial}{\partial\tau_R}-\frac{1}{2}\gamma\left(1+m_R\frac{\partial}{\partial m_R}\right)\right]\frac{\tau_R^2}{2v_R}=-\gamma_\tau\frac{\tau_R^2}{2v_R}, \tag{76}$$

using Eqs. (58) and (71) and combining Eqs. (74) and (76).

Solving Eq. (75) is then standard. At the fixed point at which $\beta(u_R^*)=0$, γ, γ_λ, and $\overline{\gamma}_\tau$ become constants marked by stars, the solution is

$$\overline{K}_R(\omega,\lambda_R,\tau_R,m_R,u_R,\mu)=\kappa^{\frac{d+2-\gamma^*}{2}}\overline{K}_R\left[(\omega/\lambda_R)\kappa^{2+\gamma_\lambda^*},\tau_R\kappa^{-2+\overline{\gamma}_\tau^*},m_R\kappa^{-\frac{d-2+\gamma^*}{2}},u_R,\mu\right]. \tag{77}$$

Employing the usual definitions of instability exponents,

$$\eta=\gamma^*,\quad \beta/\nu=(d-2+\eta)/2,$$
$$z=2+\gamma_\lambda^*,\quad 1/\nu=2-\overline{\gamma}_\tau^*,$$
$$\beta\delta/\nu=(d+2-\eta)/2, \tag{78}$$

we can write Eq. (77) in the familiar form

$$\overline{K}_R(\lambda_R,\tau_R,m_R)=\kappa^{\beta\delta/\nu}\overline{K}_R(\lambda_R t\kappa^z,\tau_R\kappa^{-1/\nu},m_R\kappa^{-\beta/\nu}), \tag{79}$$

where we have used identical symbols for variables in both the time and the frequency domains. Near an instability point, we can solve m_R from Eq. (79) and obtain

$$m_R(\lambda_R,\tau_R,\overline{K}_R)=\kappa^{\beta/\nu}m_R(\lambda_R t\kappa^z,\tau_R\kappa^{-1/\nu},\overline{K}_R\kappa^{-\beta\delta/\nu}). \tag{80}$$

One sees that the scaling form (80) is similar to Eq. (27) and K_R and $\tau_R^2/(2v_R)$ are automatically combined together as a single variable in the solution. However, Eq. (80) contains τ_R as an independent variable, which is incorrect. RG theory cannot tell us why this variable must be absent. If we omit it, we have a correct scaling form that verifies Eq. (27).

From Eq. (71), one finds that, at the fixed point [39],

$$\beta(u_R^*)=-u_R^*\left(\frac{\epsilon}{2}-\frac{3}{2}\gamma^*+\gamma_\tau^*\right)=0. \tag{81}$$

This gives rise to the exact relation

$$\gamma_\tau^* = \frac{3}{2}\gamma^* - \frac{\epsilon}{2}, \tag{82}$$

which reflects the relationship between the renormalization factors. As a result, we have exactly

$$\begin{aligned} &1/\nu = 2 - (\gamma^* - \gamma_\tau^*) = 2 - (\epsilon - \eta)/2, \\ &\beta = \nu(d - 2 + \eta)/2 = 1 \end{aligned} \tag{83}$$

from Eqs. (71) and (78).

Using Eq. (65), we obtain

$$\beta(u_R^*) = -\epsilon u_R^*/2 - 3u_R^{*3}/4 = 0 \tag{84}$$

for the fixed points to one-loop order. One solution is the trivial Gaussian fixed point $u_R^* = 0$. The other is $u_R^{*2} = -2\epsilon/3$, which is imaginary. However, it is infrared stable [10, 11] for $\epsilon > 0$, similar to the fixed point for critical phenomena [45, 46]. From Eqs. (65), (71), (78), and (83), one obtains [10, 11]

$$\begin{aligned} &\eta = -\epsilon/9, \quad 1/\nu = 2 - 5\epsilon/9, \\ &z = 2 - \epsilon/18, \quad \delta = 2 - 7\epsilon/18, \end{aligned} \tag{85}$$

to one-loop order. All exponents are real. For $\epsilon = 0$, all the exponents recover their respective mean-field values correctly.

5.4 Renormalization group equations and their solutions for reduced theories

As we have seen from the last section, the general theory contains one redundant parameter that has to be removed manually [48]. In this section, we study the reduced theories that directly give rise to correct results.

Because of the relation (57), we can either shift the mass to the field and obtain the massless theory or vice versa and arrive at the purely massive theory similar to the mean-field approximation.

We start with the massless theory, Eq. (12) with Gaussian noise (4). Its dynamic functional is similar to Eq. (51) in the absence of τ and with $\overline{K}$ replacing K. Its RG equation is then simply

$$\left[\mu\frac{\partial}{\partial\mu} + \beta\frac{\partial}{\partial u_R} + \gamma_\lambda\lambda_R\frac{\partial}{\partial\lambda_R} - \frac{1}{2}\gamma\left(1 + m_R\frac{\partial}{\partial m_R}\right)\right]\overline{K}_R = 0, \tag{86}$$

which is similar to Eq. (75). Its solution at the infrared-stable fixed point is

$$\overline{K}_R(\lambda_R, m_R, u_R^*) = \kappa^{\beta\delta/\nu}\overline{K}_R(\lambda_R t\kappa^z, m_R\kappa^{-\beta/\nu}, u_R^*), \tag{87}$$

or, in terms of m_R,

$$m_R(\lambda_R, \overline{K}_R) = \kappa^{\beta/\nu} m_R(\lambda_R t\kappa^z, \overline{K}_R\kappa^{-\beta\delta/\nu}), \tag{88}$$

which is the scaling form (27) with a momentum instead of a length rescaling factor.

Now we turn to the purely massive theory, Eq. (14) with Gaussian noise (4). Its dynamic functional is again similar to Eq. (51) now in the absence of K and with $\overline{\tau}$ replacing τ. Its RG equation can be obtained from $m_R = G_R^{(10)}(\{\mathbf{0}, 0\}; \lambda_R, \tau_R, u_R, \mu)$. It is

$$\left(\mu\frac{\partial}{\partial\mu} + \beta\frac{\partial}{\partial u_R} + \gamma_\lambda\lambda_R\frac{\partial}{\partial\lambda_R} + \gamma_{\overline{\tau}}\overline{\tau}_R\frac{\partial}{\partial\overline{\tau}_R} + \frac{1}{2}\gamma\right)m_R = 0, \tag{89}$$

with an additional Wilson function

$$\gamma_{\overline{\tau}}(u_R) = \mu\frac{\partial\ln\overline{\tau}_R}{\partial\mu} = \gamma - \frac{1}{2}\gamma_\tau \tag{90}$$

from Eqs. (67) and (71). Equation (89) can also be obtained by assuming that m_R is a function of the other variables. The fixed-point solution is then

$$m_R(\lambda_R, \overline{\tau}_R, u_R^*) = \kappa^{\beta/\nu} m_R(\lambda_R t\kappa^z, \overline{\tau}_R\kappa^{-1/\overline{\nu}}, u_R^*), \tag{91}$$

with

$$1/\overline{\nu} = 2 - \gamma^* + \gamma_\tau^*/2 \tag{92}$$

from the fixed-point solution of Eq. (90). Equation (91) is just another scaling form of (31) and thus confirms the latter. Using the exact relation (82) and the definition (78), we find

$$\overline{\nu} = 4/(d + 2 - \eta) = 2\nu/(\beta\delta). \tag{93}$$

This is just the relation that we obtained from the scaling theories and promised to prove.

Relation (93) is, as mentioned, surprising because $\overline{\tau}$ appears proportional to τ from its definition (15). However, this might be expected because $\overline{\tau}^2$ is proportional to $\overline{K}$ again from their definitions and thus shares with the latter identical anomalous dimensions. Indeed, from Eqs. (91) and (93), the exponent for $\overline{\tau}^2$ is just $2/\overline{\nu}$ and is thus $\beta\delta/\nu$, the exponent for $\overline{K}$, as seen from Eq. (88). The proportional coefficient, $2v$, between $\overline{\tau}$ and $\overline{K}$, as seen from Eqs. (13) and (15), just compensates for the difference in their naive dimensions.

Using Eqs. (83) and (85), we find

$$\overline{\nu} = \frac{1}{2}\left(1 + \frac{17}{36}\epsilon\right) \tag{94}$$

to one-loop order. The mean-field result is thus 1/2, which is equal to ν as mentioned.

For the purely thermal models including the generalized one, one just needs to replace $\overline{\tau}$ with τ itself. The fixed-point solution is simply

$$m_R(\lambda_R, \tau_R, u_R^*) = \kappa^{\beta/\nu} m_R(\lambda_R t\kappa^z, \tau_R \kappa^{-1/\nu}, u_R^*), \quad (95)$$

which is just Eq. (80) of the general theory without $\overline{K}$. However, as has been pointed out in Section 5.1, the purely thermal model with $\sigma = 2$ itself does not correctly describe the temperature-driven FOPTs. For the generalized model, the renormalization factors are different from the φ^3 ones, though the symbols for the exponents are identical.

5.5 Thermal hysteresis exponents

RG theories have confirmed the scaling forms developed in Section 4. They also yield the ϵ expansions for the hysteresis exponents. The relation (93) has also confirmed the identity of the two sets of exponents obtained from the two reduced theories. Therefore, we shall only consider the hysteresis exponents of the massless theory, Eqs. (36), (39), and (47), and of the purely thermal theory, Eq. (48).

Using Eqs. (78) and (83), we can write the hysteresis exponents for the three thermal classes as

$$\Upsilon = \frac{\beta\delta}{\beta\delta + \nu z} = \frac{d + 2 - \eta}{d + 2 - \eta + 2z}, \quad (96)$$

$$\Upsilon_m = \frac{\beta}{\beta\delta + \nu z} = \frac{d - 2 + \eta}{d + 2 - \eta + 2z}, \quad (97)$$

$$\dot{\Upsilon} = \frac{\beta\delta}{\beta\delta + 2\nu z} = \frac{d + 2 - \eta}{d + 2 - \eta + 4z}, \quad (98)$$

$$\dot{\Upsilon}_m = \frac{2\beta}{\beta\delta + 2\nu z} = \frac{2(d - 2 + \eta)}{d + 2 - \eta + 4z}, \quad (99)$$

$$\ddot{\Upsilon} = \ddot{\Upsilon}_m = \frac{d - 2 + \eta}{d - 2 + \eta + 2z}. \quad (100)$$

To one-loop order, these become

$$\Upsilon = \frac{2}{3}\left(1 - \frac{1}{36}\epsilon\right), \quad \dot{\Upsilon} = \frac{1}{2}\left(1 - \frac{1}{24}\epsilon\right),$$
$$\Upsilon_m = \frac{1}{3}\left(1 - \frac{7}{36}\epsilon\right), \quad \dot{\Upsilon}_m = \frac{1}{2}\left(1 - \frac{5}{24}\epsilon\right) \quad (101)$$

from Eq. (85). We have not listed $\ddot{\Upsilon}$ and $\ddot{\Upsilon}_m$ as they do not describe the temperature-driven transitions for $\sigma = 2$. Nevertheless, to one-loop order, they are $\ddot{\Upsilon} = \ddot{\Upsilon}_m = 1/2 - \epsilon/18$, which are indeed different from those of Thermal Class II beyond the mean-field level. The field-like hysteresis exponents are in fact identical to the field-driven FOPTs as mentioned and have been given in Ref. [11]. The thermal-like exponents are the result of the present study.

The estimates of the hysteresis exponents can be further improved. By utilizing the three- and two-loop results of the static [58, 59] and dynamic [39] exponents for the Yang–Lee edge singularity and some exact results in low dimensions [15], Padé resummations have been performed and the best estimates for η and z up to date have been presented [11]. From these results, similar estimates for the hysteresis exponents in Eqs. (96)–(100) can also be computed. These results all listed in Table 1. Included in the last two rows are the results of the general purely thermal class for $\sigma = 3$, the ϕ^6 model studied in Section 4.3. These exponents are extracted directly from Ref. [40], where they are the hysteresis exponents for nonequilibrium *critical* phenomena of the Ising universality class, because the two models are of the same universality class.

The mean-field hysteresis exponents listed in Table 1 have been confirmed numerically. The hysteresis exponents listed explicitly for $d = 0$ are exact because, in this dimension, $z = (2 - \eta)/2$ [39]. The hysteresis exponents for the purely thermal class with $\sigma = 3$ in $d = 2$ have been verified numerically [40] and so have those for the

Table 1 Instability exponents and thermal hysteresis exponents.*

d		6	5	4	3	2	1	0
η	[11]	0	-0.147 ± 0.002	$-0.329^{+0.012}_{-0.013}$	$-0.527^{+0.029}_{-0.033}$	$-0.747^{+0.064}_{-0.050}$	-1 [15]	-1.224
z	[11]	2	1.941 ± 0.003	1.880 ± 0.006	1.817 ± 0.008	1.753 ± 0.010	1.677	1.612
Υ	Thermal Class I [11]	2/3	0.6480 ± 0.0004	0.627 ± 0.001	0.603 ± 0.003	0.575 ± 0.004	0.544	1/2
Υ_m	Thermal Class I [11]	1/3	0.259 ± 0.0003	0.166 ± 0.002	$0.0516^{+0.0031}_{-0.0035}$	$-0.0905^{+0.0047}_{-0.0062}$	-0.272	$-1/2$
$\dot{\Upsilon}$	Thermal Class II	1/2	0.4793 ± 0.0005	0.457 ± 0.002	0.432 ± 0.003	0.404 ± 0.004	0.374	1/3
$\dot{\Upsilon}_m$	Thermal Class II	1/2	0.3827 ± 0.0005	$0.241^{+0.002}_{-0.003}$	$0.0739^{+0.005}_{-0.006}$	$-0.127^{+0.007}_{-0.009}$	-0.374	$-2/3$
$\ddot{\Upsilon} = \ddot{\Upsilon}_m$	Thermal Class III	1/2	—	—	—	—	—	—
$\ddot{\Upsilon}$	$\sigma = 3$ [40]	1/2	1/2	1/2	0.4380(15)	0.3158(1)		
$\ddot{\Upsilon}_m$	$\sigma = 3$ [40]	1/2	1/2	1/2	0.1430(49)	0.03948(2)		

*quoted errors reflect the spread in different resummations except the last two rows.

field-like class for $d = 7$–4 [60]. The remaining hysteresis exponents have yet to be tested.

Experimentally, the mean-field exponent Υ has been confirmed in liquid crystals [9]. It has also been estimated to range from 0.26 to 0.49 in a couple of alloys and compounds [1–6], which is not far from the theoretically value for $d = 3$. However, the ranges of the sweep rate R employed in these experiments are small and thus further experiments are desirable.

6 Summary

We have studied the scaling and universal behavior of temperature-driven FOPTs. We have shown that these transitions exhibit rich phenomena though they are controlled by a single complex-conjugate pair of imaginary fixed points of ϕ^3 theory.

The expansion near the spinodal or instability point of an FOPT results in a leading ϕ^3 theory. Its shift symmetry leads to two equivalent reduced models: a massless model (12) and a purely massive model (14). Although the latter is real only in the absence of an external field and under cooling, in which case it becomes a purely thermal model (16) or its generalizations (17), it falls into the same universality class as the massless model and verifies the unique properties of ϕ^3 theory. Scaling theories have also been proposed. The resultant scaling forms give rise to several universality classes with their own hysteresis exponents. These include the field-like Thermal Class I, the partly thermal class Thermal Class II, and the purely thermal class Thermal Class III. The first two classes are opposite limits of the scaling forms and may crossover to each other depending on the temperature sweep rate R. They are both described by the massless model and the purely massive model. The last class is characterized by purely thermal models and contains different universality classes depending on the symmetry of the order parameters. An example is the ϕ^6 model whose cooling transition in the absence of an applied external field falls into the same universality class as the nonequilibrium critical phenomena of the usual ϕ^4 model. If odd-symmetry terms are allowed in the free energies, Thermal Class III emerges only in the mean-field limit and is identical to Thermal Class II. It changes to the other two classes when fluctuations are considered. Numerical and analytical results at the mean-field level agree well with the scaling analysis. Renormalization group theories confirm both the scaling theory and the relation between the massless model and the purely massive model and provide methods to calculate the hysteresis exponents of various universality classes. Using the extant three- and two-loop results for the static and dynamic exponents for the Yang–Lee edge singularity, which falls into the same universality class as ϕ^3, we have estimated the thermal hysteresis exponents of the various classes to the same precision. A few exponents have already been verified both numerically and experimentally and further comparisons are desirable.

Acknowledgements We thank Shuai Yin and Baoquan Feng for their helpful discussions. This work was supported by the National Natural Science foundation of PRC (Grants Nos. 10625420 and 11575297) and FRFCUC.

References and notes

1. Z. C. Lin, K. F. Liang, W. G. Zeng, and J. X. Zhang, Dynamic equation and characteristic internal frictions of mobile interfaces in phase transitions, in: Internal Friction and Ultrasonic Attenuation, eds. T. S. Ke and L. D. Zhang, Beijing: Atomic Energy Press of China, 1989, p. 87
2. K. F. Liang, Z. C. Lin, P. C. W. Fung, and J. X. Zhang, Characterization of the thermoelastic martensitic transformation in a NiTi alloy driven by temperature variation and external stress, *Phys. Rev. B* 56(5), 2453 (1997)
3. See, e. g., J. X. Zhang, F. Zhong, and G. G. Siu, The scanning-rate dependence of energy dissipation in first-order phase transition of solids, *Solid State Commun.* 97(10), 847 (1996)
4. J. Liu and J. X. Zhang, Temperature-rate dependent kinetics of martensitic transformation in MnCu alloy, *Solid State Commun.* 98(6), 539 (1996)
5. P. C. W. Fung, J. X. Zhang, Y. Lin, K. F. Liang, and Z. C. Lin, Analysis of dissipation of a burst-type martensite transformation in a Fe-Mn alloy by internal friction measurements, *Phys. Rev. B* 54(10), 7074 (1996)
6. Z. Q. Kuang, J. X. Zhang, X. H. Zhang, K. F. Liang, and P. C. W. Fung, Scaling behaviours in the thermoelastic martensitic transformation of Co, *Solid State Commun.* 114(4), 231 (2000)
7. M. Rao and R. Pandit, Magnetic and thermal hysteresis in the $O(N)$-symmetric $(\phi^2)^3$ model, *Phys. Rev. B* 43(4), 3373 (1991)
8. F. Zhong and J. X. Zhang, Scaling of thermal hysteresis with temperature scanning rate, *Phys. Rev. E* 51(4), 2898 (1995)
9. S. Yıldız, Ö. Pekcan, A. N. Berker, and H. Özbek, Scaling of thermal hysteresis at nematic-smectic-A phase transition in a binary mixture, *Phys. Rev. E* 69(3), 031705 (2004)
10. F. Zhong, and Q. Z. Chen, Theory of the dynamics of first-order phase transitions: Unstable fixed points, exponents, and dynamical scaling, *Phys. Rev. Lett.* 95(17), 175701 (2005)
11. F. Zhong, Renormalization-group theory of first-order phase transition dynamics in field-driven scalar model, *Front. Phys.* 12, 126403 (2017)

12. F. Zhong, Imaginary fixed points can be physical, *Phys. Rev. E* 86(2), 022104 (2012)
13. S. Fan and F. Zhong, Evidences of the instability fixed points of first-order phase transitions, *J. Stat. Phys.* 143(6), 1136 (2011)
14. Y. T. Li and F. Zhong, Functional renormalization group approach to the dynamics of first-order phase transitions, arXiv: 1111.1573 (2011)
15. M. E. Fisher, Yang–Lee edge singularity and ϕ^3 field theory, *Phys. Rev. Lett.* 40(25), 1610 (1978)
16. J. D. Gunton and D. Droz, Introduction to the Theory of Metastable and Unstable States, Berlin: Springer, 1983
17. J. D. Gunton, M. San Miguel, and P. S. Sahni, in: Phase Transitions and Critical Phenomena, eds. C. Domb and J. L. Lebowitz, Vol. 8, London: Academic, 1983
18. K. Binder, Theory of first-order phase transitions, *Rep. Prog. Phys.* 50(7), 783 (1987)
19. K. Binder and P. Fratzl, in: Phase Transformations in Materials, ed. G. Kostorz, Weinheim: Wiley, 2001
20. K. Binder, C. Billotet, and P. Mirold, On the theory of spinodal decomposition in solid and liquid binary mixtures, *Z. Phys. B* 30(2), 183 (1978)
21. C. Billotet and K. Binder, Nonlinear relaxation at first-order phase transitions: A Ginzburg–Landau theory including fluctuations, *Z. Phys. B* 32(2), 195 (1979)
22. K. Kawasaki, T. Imaeda, and J. D. Gunton, in: Perspectives in Statistical Physics, ed. H. J. Raveché, Amsterdam: North Holland, 1981, p. 201
23. K. Kaski, K. Binder, and J. D. Gunton, A study of a coarse-grained free energy functional for the three-dimensional Ising model, *J. Phys. A* 16(16), L623 (1983)
24. K. Kaski, K. Binder, and J. D. Gunton, Study of cell distribution functions of the three-dimensional Ising model, *Phys. Rev. B* 29(7), 3996 (1984)
25. D. W. Heermann, W. Klein, and D. Stauffer, Spinodals in a long-range interaction system, *Phys. Rev. Lett.* 49, 1262 (1982)
26. N. Gulbahce, H. Gould, and W. Klein, Zeros of the partition function and pseudospinodals in long-range Ising models, *Phys. Rev. E* 69(3), 036119 (2004)
27. J. S. Langer, Theory of the condensation point, *Ann. Phys.* 41(1), 108 (1967)
28. W. Klein and C. Unger, Pseudospinodals, spinodals, and nucleation, *Phys. Rev. B* 28(1), 445 (1983)
29. C. Unger and W. Klein, Nucleation theory near the classical spinodal, *Phys. Rev. B* 29(5), 2698 (1984)
30. D. W. Oxtoby, Homogeneous nucleation: Theory and experiment, *J. Phys.: Condens. Matter* 4(38), 7627 (1992)
31. P. B. Thomas and D. Dhar, Hysteresis in isotropic spin systems, *J. Phys. A* 26(16), 3973 (1993)
32. S. W. Sides, P. A. Rikvold, and M. A. Novotny, Stochastic hysteresis and resonance in a kinetic Ising system, *Phys. Rev. E* 57(6), 6512 (1998)
33. S. W. Sides, P. A. Rikvold, and M. A. Novotny, Kinetic Ising model in an oscillating field: Avrami theory for the hysteretic response and finite-size scaling for the dynamic phase transition, *Phys. Rev. E* 59(3), 2710 (1999)
34. M. Acharyya and B. K. Chakrabarti, Response of Ising systems to oscillating and pulsed fields: Hysteresis, ac, and pulse susceptibility, *Phys. Rev. B* 52(9), 6550 (1995)
35. L. D. Landau and E. M. Lifshitz, Statistical Physics, Ch. XIV, Oxford: Pergamon, 1986
36. P. G. de Gennes, Short range order effects in the isotropic phase of nematics and cholesterics, *Mol. Cryst. Liq. Cryst.* 12(3), 193 (1971)
37. A. F. Devonshire, Theory of barium titanate (Part I), *Phil. Mag.* 40, 1040 (1949); A. F. Devonshire, Theory of barium titanate (Part II), *Phil. Mag.* 42, 1065 (1951)
38. P. C. Hohenberg, and B. I. Halperin, Theory of dynamic critical phenomena, *Rev. Mod. Phys.* 49(3), 435 (1977)
39. N. Breuer and H. K. Janssen, Equation of state and dynamical properties near the Yang–Lee edge singularity, *Z. Phys. Condensed Matter* 41(1), 55 (1981)
40. F. Zhong, Probing criticality with linearly varying external fields: Renormalization group theory of nonequilibrium critical dynamics under driving, *Phys. Rev. E* 73(4), 047102 (2006)
41. S. Gong, F. Zhong, X. Huang, and S. Fan, Finite-time scaling via linear driving, *New J. Phys.* 12(4), 043036 (2010)
42. F. Zhong, Finite-time scaling and its applications to continuous phase transitions, in Applications of Monte Carlo Method in Science and Engineering, ed. S. Mordechai, p. 469, Rijeka: Intech, 2011. Available at http://www.intechopen.com/articles/show/title/finite-time-scaling-and-its-applications-to-continuous-phase-transitions
43. CRC Standard Mathematical Tables & Formulae, ed. D. Zwillinger, 30th Ed., Florida: CRC, 1996
44. P. Jung, G. Gray, R. Roy, and P. Mandel, Scaling law for dynamical hysteresis, *Phys. Rev. Lett.* 65(15), 1873 (1990)
45. J. Zinn-Justin, Quantum Field Theory and Critical Phenomena, 3rd Ed., Oxford: Clarendon, 1996
46. D. J. Amit and V. Martin-Mayor, Field Theory, the Renormalization Group, and Critical Phenomena, 3nd Ed., Singapore: World Scientific, 2005
47. H. Kleinert and V. Schulte-Frohlinde, Critical Properties of ϕ^4-Theory, Singapore: World Scientific, 2001
48. A. N. Vasil'ev, The Field Theoretic Renormalization Group in Critical Behavior Theory and Stochastic Dynamics, London: Chapman and Hall/CRC, 2004
49. F. J. Wegner and E. K. Riedel, Logarithmic corrections to the molecular-field behavior of critical and tricritical systems, *Phys. Rev. B* 7(1), 248 (1973)

50. K. G. Wilson and J. Kogut, The renormalization group and the ε expansion, *Phys. Rep.* 12(2), 75 (1974)
51. S. K. Ma, Modern Theory of Critical Phenomena, Benjamin, 1976
52. H. K. Janssen, in: Dynamical Critical Phenomena and Related topics, Lecture Notes in Physics, Vol. 104, ed. C. P. Enz, Berlin: Springer, 1979
53. H. K. Janssen, in: From Phase Transition to Chaos, edited by G. Györgyi, I. Kondor, L. Sasvári, and T. Tél, Singapore: World Scientific, 1992
54. U. C. Täuber, Critical Dynamics, http://www.phys.vt.edu/∼tauber/utaeuber.html
55. P. C. Martin, E. D. Siggia, and H. A. Rose, Statistical dynamics of classical systems, *Phys. Rev. A* 8(1), 423 (1973)
56. G. 't Hooft and M. Veltman, Regularization and renormalization of gauge fields, *Nucl. Phys. B* 44(1), 189 (1972)
57. C. De Dominicis and L. Peliti, Field-theory renormalization and critical dynamics above T_c: Helium, antiferromagnets, and liquid-gas systems, *Phys. Rev. B* 18(1), 353 (1978)
58. O. F. A. Bonfim, J. E. Kirkham, and A. J. McKane, Critical exponents to order ϵ^3 for ϕ^3 models of critical phenomena in 6-ϵ dimensions, *J. Phys. Math. Gen.* 13(7), L247 (1980)
59. O. F. A. Bonfirm, J. E. Kirkham, and A. J. McKane, Critical exponents for the percolation problem and the Yang–Lee edge singularity, *J. Phys. Math. Gen.* 14(9), 2391 (1981)
60. J. Yu, Scaling of first-order phase transition dynamics, Master thesis, Sun Yat-sen University, 2012 (unpublished)